Selection of hammerhead ribozymes for optimum cleavage of interleukin 6 mRNA

Chris HENDRIX*, Jozef ANNÉ†, Bernard JORIS‡, Arthur VAN AERSCHOT* and Piet HERDEWIJN*§

*Laboratory for Medicinal Chemistry and †Laboratory for Bacteriology, Rega Institute, K.U. Leuven, Minderbroedersstraat 10, B-3000 Leuven, Belgium, and ‡Center for Protein Engineering, University of Liège, B-4000 Sart-Tilman-Liège 1, Belgium

Four GUC triplets in the coding region of the mRNA of interleukin 6 (IL-6) were examined for their suitability to serve as a target for hammerhead ribozyme-mediated cleavage. This selection procedure was performed with the intention to down-regulate IL-6 production as a potential treatment of those diseases in which IL-6 overexpression is involved. Hammerhead ribozymes and their respective short synthetic substrates (19-mers) were synthesized for these four GUC triplets. Notwithstanding the identical catalytic core sequences, the difference in base composition of the helices involved in substrate binding caused substantial variation in cleavage activity. The cleavage reactions on the 1035 nucleotide IL-6 mRNA transcript revealed that two ribozymes were able to cleave this substrate, showing a decrease in catalytic efficiency to 1/30 and 1/300 of the short substrate. This study indicates that the GUC triplet located at nucleotide 510 of the mRNA of IL-6 is the best site for hammerhead ribozyme-mediated cleavage. We suggest that in future targeting of chemically modified hammerhead ribozymes for cleavage of IL-6 mRNA should be directed at this location.

INTRODUCTION

Interleukin 6 (IL-6) is one of the most pleiotropic cytokines yet discovered. It is involved mainly in coordinating functions during haematopoiesis, immune regulation and the acute-phase response [1]. IL-6 has the capacity to cause clinical abnormalities, directly or indirectly, by non-physiological overproduction. It has been implicated in the pathogenesis of several cancers and diseases such as rheumatoid arthritis, Castleman's disease, multiple myeloma, AIDS, Kaposi's sarcoma, systemic lupus erythematosus, cardiac myxoma and mesangioproliferative glomerulonephritis [2,3,4]. Down-regulation of the IL-6 production might therefore be a good strategy for combating life-threatening and otherwise unacceptable levels of IL-6.

A promising new direction in the search for pharmaceutical agents has been opened by the discovery of several classes of ribozymes, which represent an advanced class of antisense molecules as they combine the substrate sequence specificity of complementary nucleic acids with the potential to degrade susceptible substrate RNAs catalytically. When using phosphodiester antisense oligonucleotides this function is normally performed by RNase H. The hammerhead ribozyme catalyses the site-specific cleavage of the substrate RNA in the presence of a divalent metal ion, preferentially Mg^{2+} or Mn^{2+}, generating a 2′,3′-cyclic phosphate [5]. These hammerhead ribozymes could be valuable in therapy because they can theoretically be developed to cleave any undesired RNA containing a triplet amenable to cleavage [6,7].

Recently Mahieu et al. [8] designed a hammerhead ribozyme, prepared by transcription *in vitro*, that cleaves IL-6 mRNA in human amniotic UAC cells. Those authors studied a single site of cleavage after the amenable GUC sequence located at nucleotide 510 of IL-6 mRNA (numbered according to the SWISS-PROT Data Bank [9]). However, human IL-6 mRNA contains four GUC sequences in the coding region, each of which is a potential target for hammerhead ribozyme-mediated cleavage. This triplet is considered to be the prime target sequence for hammerhead ribozymes [6,7]. Here we report the synthesis of hammerhead ribozymes, directed against these four GUC sequences, and compare the cleavage activity towards short synthetic substrates with their activity on the long mRNA substrate. We studied the most probable secondary structure of the ribozymes, the short substrates and the IL-6 mRNA and the melting temperatures of the complexes formed between the ribozymes and their respective short synthetic substrates in order to explain the difference in activity.

EXPERIMENTAL

Materials and methods

Tetrabutylammonium fluoride (1 M in tetrahydrofuran) was purchased from Acros Chimica. Long-chain alkylamine controlled-pore glass (LCAA-CPG), supplied by Pierce, was functionalized with 1-*O*-dimethoxytrityl-1,3-propanediol analogously to the protocol reported by Tang et al. [10]. The short substrate oligoribonucleotides were ^{32}P-labelled at the 5′ end with T4 polynucleotide kinase (Gibco BRL) and [γ-^{32}P]ATP (4500 Ci/mmol; ICN) and purified on a NAP-10 column (Pharmacia). Nucleoside triphosphates were purchased from Sigma; [α-^{32}P]UTP (3000 Ci/mmol) was from ICN. All other chemicals were of analytical grade.

Oligoribonucleotides were synthesized on an Applied Biosystems 392 DNA Synthesizer on a 1–2 μmol scale by using phosphoramidites from Milligen Biosearch. The oligoribonucleotides were worked up as described previously [11]. Scanning laser densitometry was performed with a DeskTop Densitometer (pdi, New York, U.S.A.) equipped with The Discovery Series (Diversity One) software.

Plasmid

The pT7.7/IL-6 expression plasmid [12], containing the IL-6 sequence, was a gift from M. Mahieu (Institut Pasteur du Brabant, Brussels).

Abbreviations used: IFN-β2, interferon β2; IL-6, interleukin 6; LCAA-CPG, long-chain alkylamine controlled-pore glass; Rib, ribozyme; Sub, substrate; T_m: melting temperature.

§ To whom correspondence should be sent. Tel or Fax: 32-16-337387.

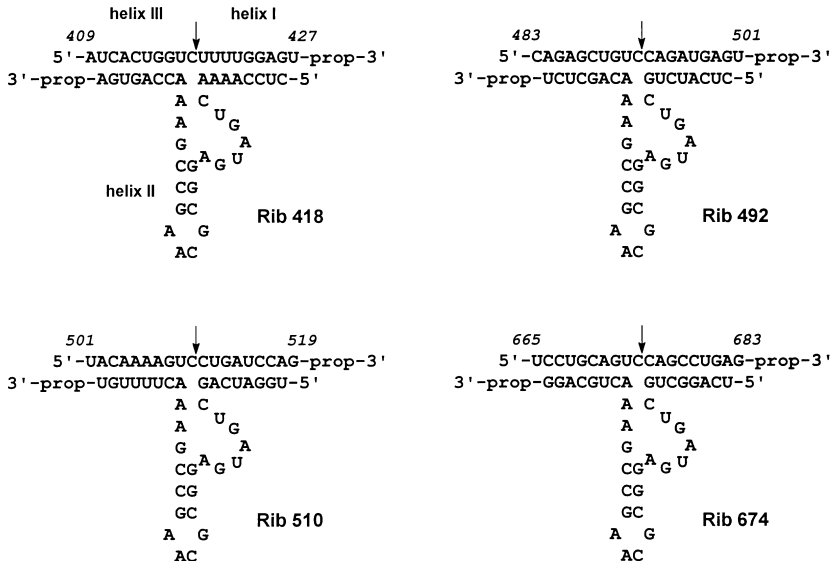

Figure 1 Structures of synthetic ribozyme–substrate complexes for the GUC sequences found in the coding region of the mRNA of IL-6

The numbers at the top of each structure indicate the position [9] of the short synthetic substrates in the coding region of IL-6 mRNA. The three RNA helices I, II and III are numbered in accordance with [31].

Enzymes

T4 polynucleotide kinase (10 units/μl) was purchased from Gibco BRL. *Sal*I (12 units/μl), Ribonuclease inhibitor (110 units/μl), T7 RNA polymerase (20 units/μl) and deoxyribonuclease I (25 units/μl) were supplied by Amersham.

Run-off transcription

pT7.7/IL-6 was linearized by *Sal*I digestion, extracted with phenol/chloroform, eluted over a Sephadex-G50 column (Pharmacia) and precipitated with ethanol. The pellet was dissolved in water and stored at -20 °C. The run-off transcription mixture (100 μl) contained 4 μg of linearized pT7.7/IL-6 DNA, 10 mM dithiothreitol, 500 μM concentrations of each rNTP, 40 mM Tris/HCl, pH 7.5, 2 mM spermidine, 6 mM $MgCl_2$, 5 mM NaCl, 5 μl of [α-^{32}P]UTP (3000 Ci/mmol, 10 mCi/ml), 1 μl of ribonuclease inhibitor (110 units/μl), 0.01 % BSA and 200 units of T7 RNA polymerase. After incubation for 90 min at 37 °C, 100 units of DNase were added and the mixture was incubated for 15 min at 37 °C. After extraction with phenol/chloroform the water phase was eluted on a NAP-10 column and precipitated with ethanol.

Cleavage kinetics with short synthetic substrate

The comparative time course of the cleavage reaction for the complexes formed between the ribozymes and their respective short synthetic substrates (19-mers) was performed with 30 nM ribozyme and 200 nM substrate. The ribozyme and the short oligoribonucleotide substrate were incubated together at 75 °C for 3 min in 50 mM Tris/HCl, pH 7.5, followed by incubation for 5 min at 30 °C. Reactions were started by the addition of an equal volume of 40 mM $MgCl_2$ in 50 mM Tris/HCl, pH 7.5, which gave a final concentration of $MgCl_2$ of 20 mM. Cleavage reactions were performed at 30 °C in a total volume of 50 μl. Aliquots were taken at appropriate times between 10 and 180 min. Reactions were stopped by the addition of an equal volume of stop mix (50 mM EDTA, 0.1 % xylene cyanol and 0.1 % Bromophenol Blue (w/v) in 90 % formamide (v/v)) and analysed by denaturing PAGE (20 % gel; 7.5 cm long) containing 8.3 M urea, followed by autoradiography. The catalytic activity of the hammerhead structures as a function of time was determined by scanning laser densitometry.

Kinetic constants, $k_{cat.}$ and K_m, for the cleavage of short synthetic substrates were determined from Eadie–Hofstee and Lineweaver–Burk plots [13] from initial velocities under multiple turnover conditions. The cleavage reactions were performed under the conditions described above with concentrations of substrate between 50 and 350 nM; ribozyme concentrations were between 5 and 30 nM. Aliquots were taken at appropriate times between 1 and 40 min.

Cleavage kinetics with IL-6 mRNA

$k_{react.}/K_m$ values were determined under single turnover conditions as described by Heidenreich et al. [14,15], by using 10 nM of long substrate (IL-6 mRNA) and between 50 and 1000 nM of ribozyme. The ribozyme was incubated at 75 °C for 3 min in 50 mM Tris/HCl, pH 7.5, after which $MgCl_2$ was added to a final concentration of 20 mM, followed by incubation for 5 min at 30 °C. Reactions were started by the addition of IL-6 mRNA. Cleavage reactions were performed at 30 °C in a total volume of 10 μl. After 1 h the reaction was stopped by addition of an equal volume of the above-mentioned stop mix, chilled on ice and analysed by denaturing PAGE (4 % gel; 20 cm long) containing 8.3 M urea, followed by autoradiography and scanning laser densitometry. Kinetic constants were obtained by plotting the observed cleavage rate $k_{obs.}$ against the quotient of $k_{obs.}$ over the ribozyme concentration, as described by Heidenreich et al. [15].

All kinetic results are the averages of at least three independent experiments. For any given ribozyme, the kinetic constants $k_{cat.}$, K_m and $k_{cat.}/K_m$ varied by a factor of approx. 2.

Melting temperatures

Melting curves were measured and evaluated as described in [16]. Oligomer concentrations were determined as described [16], with an extinction coefficient of 10000 for uridine at 80 °C.

Secondary structure

The most probable secondary structure of the mRNA of IL-6 was determined by the method of Zuker [17] by using the FOLDRNA and SQUIGGLES software included in the Wisconsin Sequence Analysis Package (Genetic Computer Group Inc.). The secondary structure of the ribozymes and the short synthetic substrates was calculated by the PC/Gene software (Intelligenetics Inc.), release 6.80.

RESULTS

The coding region of the mRNA of IL-6 contains four GUC sequences, which are potential targets for cleavage by a hammerhead ribozyme. These GUC triplets were selected on the human IL-6 mRNA sequence, provided by the SWISS-PROT Data Bank (HSIFNβ2, M14584) [9] and are located at nucleotides 418, 492, 510 and 674 (position of C). The triplet at nucleotide 492, coding for valine, has also been published as being GUG instead of GUC [18], which is in contradiction with the sequence provided by the data bank [9]. Brakenhoff et al. [19] compared the cDNA sequences of hybridoma growth factor, interferon β2 (IFN-β2), 26,000 protein and B-cell stimulatory factor 2, which are different names for the same molecule, IL-6, each reflecting a different characteristic of the protein. This comparison revealed that the GUC in IFN-β2 is a GUG in the other three sequences and that this might be a reflection of polymorphism. Our mRNA transcript, obtained from the pT7.7/IL-6 plasmid [12], also has a GUG at that position. Unfortunately, GUG is the only combination of the amenable triplet NUX, N and X being any nucleotide, which is not a target for hammerhead ribozymes [6,7]. Nevertheless we included this target in our study for the cleavage of the short substrates and to serve as a control ribozyme for the long substrate (no cleavage activity on IL-6 mRNA) and we intend to keep it in mind for future studies *in vivo*.

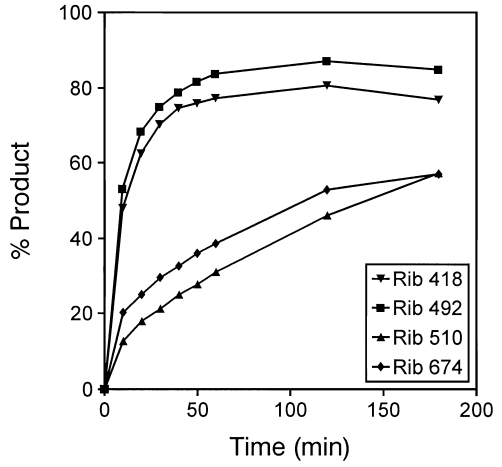

Figure 2 Percentage of product plotted against time for the cleavage reaction of the hammerhead ribozymes with their respective short synthetic substrates

The comparative cleavage reactions were performed by treating 200 nM short synthetic substrate with 30 nM ribozyme at 30 °C in the presence of 20 mM $MgCl_2$, as described in the Experimental section.

For these four targets we synthesized hammerhead ribozymes (36-mers: Rib 418, Rib 492, Rib 510 and Rib 674) and the respective short synthetic substrates (19-mers: Sub 418, Sub 492, Sub 510 and Sub 674). Their sequences are shown in Figure 1. The helix and loop II of the ribozymes consisted of three base pairs attached to a thermodynamically stable tetraloop GCAA [20,21]. For all the oligoribonucleotides, 1-*O*-dimethoxytrityl-1,3-propanediol-functionalized LCAA-CPG, synthesized analogously to the synthesis reported by Tang et al. [10], was used as a universal solid phase. By means of this solid phase a propanediol group, rendering improved stability towards 3′-exonucleolytic attack [22,23], was attached at the 3′-end.

Comparative cleavage reactions for the four complexes were performed with 30 nM of ribozyme and 200 nM ^{32}P-labelled short synthetic substrate. Earlier cleavage experiments with similar ribozymes at 25, 30 and 37 °C prompted us to use 30 °C as the incubation temperature for all the kinetic experiments, because at this temperature the best cleavage rate was obtained and at 37 °C a considerable amount of aspecific degradation of the substrate was observed [24]. The time course of the cleavage (Figure 2) shows that Rib 492 and Rib 418 have comparable cleavage activities and are far more active than Rib 510 and Rib 674, which also show similar activities. These preliminary results were confirmed by analysis of the initial velocities under multiple turnover conditions of cleavage of these short synthetic substrates (Table 1). K_m values are in the same range for the four complexes; a large difference can be observed for the $k_{cat.}$ values, which vary from 0.050 min^{-1} for Rib 674 to 0.866 min^{-1} for Rib 492.

The melting temperatures for the complexes formed between the ribozymes and their respective short synthetic substrates, determined by UV spectrometry, were nearly the same for Rib 418, Rib 492 and Rib 510, but much higher for Rib 674 (Figure

Table 1 Catalytic parameters of the different ribozymes with short synthetic substrates and the long substrate, IL-6 mRNA

Reaction conditions were as described in the Experimental section. No activity was observed on IL-6 mRNA with either Rib 492 or Rib 673.

	Short synthetic substrate			IL-6 mRNA		
Ribozyme	$k_{cat.}$ (min^{-1})	K_m (nM)	$k_{cat.}/K_m$ ($10^6 \times min^{-1} \cdot M^{-1}$)	$k_{react.}$ (min^{-1})	K_m (nM)	$k_{react.}/K_m$ ($10^6 \times min^{-1} \cdot M^{-1}$)
Rib 418	0.501	87	5.75	0.0024	125	0.019
Rib 492	0.866	80	10.83	–	–	–
Rib 510	0.142	130	1.38	0.0041	98	0.042
Rib 674	0.050	59	0.841	–	–	–

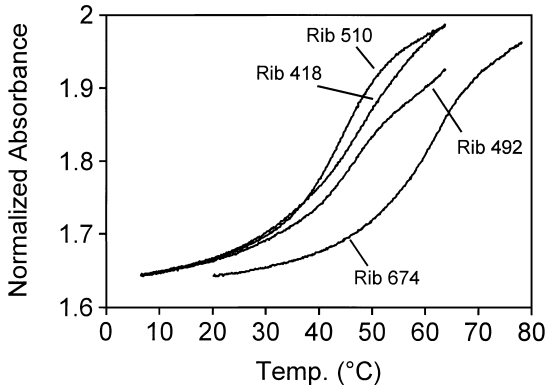

Figure 3 Melting temperature for complexes formed between the ribozymes and short synthetic substrate RNA (19-mer)

Melting temperatures were determined under the following conditions: 0.1 M NaCl, 0.02 M potassium phosphate, pH 7.5, 0.1 mM EDTA; each oligonucleotide was present at a concentration of 3 μM.

3; Table 2). This can be explained by the numbers of GC base pairs in helices I and II: 9 AU and 7 GC in Rib 418; 8 AU and 8 GC in Rib 492; 10 AU and 6 GC in Rib 510; and 6 AU and 10 GC in Rib 674.

The secondary structures of the ribozymes and the short substrates were calculated by the PC/Gene software with the RNAFOLD program, which predicts the secondary structures of RNA sequences by using the method of Zuker and Stiegler [25]. The structures, predicted by two calculation methods with the free-energy values of either Cech et al. [26] or Freier et al. [27], are shown in Figure 4. The corresponding free energies of the structures are shown in Table 2. Most of the sequences examined here gave identical secondary structures by both methods, except

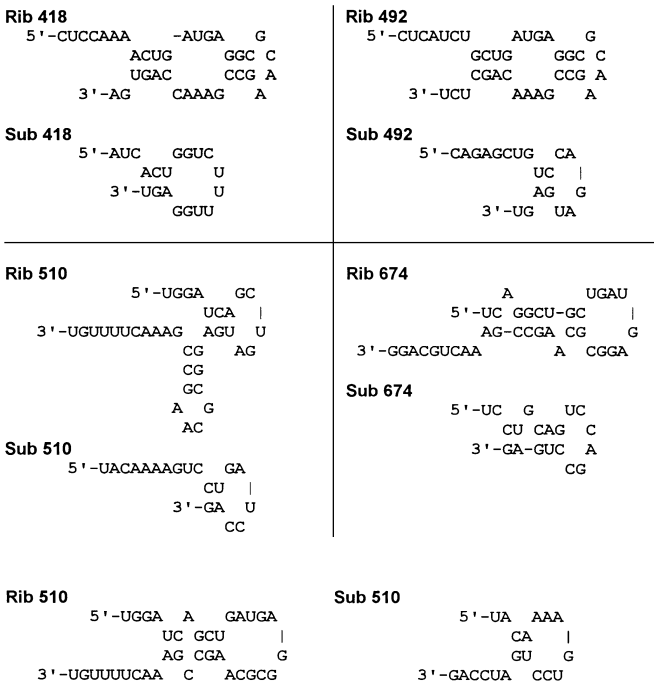

Figure 4 Secondary structures of the ribozymes and the short synthetic substrates as calculated by the PC/Gene software

The top four panels show structures calculated from free-energy values from [26]; at the bottom are shown two different structures resulting from calculations with values from [27]. The corresponding free-energy values are listed in Table 2.

for Rib 510 and Sub 510. With Freier's free-energy values, Rib 510 did not fold to the proper ribozyme structure because a correct helix and loop II were lacking. By both methods Rib 674

Table 2 Melting temperature for complexes formed between the ribozymes and short synthetic substrate RNA (19-mer) and free energy values of structures predicted by calculation with the PC/Gene software

The melting temperature is for complexes formed between the ribozymes and the short synthetic substrate, as depicted in Figure 3. Note: 1 kcal ≡ 4.184 kJ.

Oligonucleotide	Melting temperature (°C)	Free-energy values (kcal)	
		From [26]	From [27]
Rib 418	48.1	−8.1	−2.9
Rib 492	46.7	−10.4	−4.5
Rib 510	44.0	−4.7	−2.0*
Rib 674	62.2	−12.3*	−6.9*
Sub 418		0.7	0.5
Sub 492		2.0	2.1
Sub 510		2.0	2.3
Sub 674		−1.3	0
5′Rib-UUUU-Sub-3′‡:			
418		−30.0†	−17.4†
492		−29.5†	−19.0*
510		−27.0†	−15.8*
674		−37.4†	−23.3*
5′-Sub-UUUU-Rib-3′‡:			
418		−30.3†	−17.9†
492		−29.5†	−19.3*
510		−27.3†	−15.9*
674		−37.4†	−22.7*

* No folding of loop and helix II.

† Correct folding of the ribozyme–substrate complex.

‡ For the calculation of the secondary structure of the ribozyme–substrate complexes, the 3′ or 5′ end of the ribozyme was connected with its corresponding short substrate via an imaginary UUUU loop.

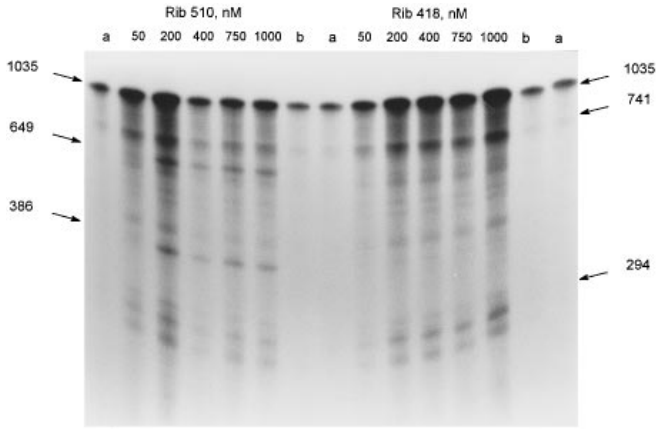

Figure 5 Cleavage of IL-6 mRNA by Rib 418 and Rib 510

The cleavage reactions with the long substrate were performed under single turnover conditions with 10 nM IL-6 mRNA and the indicated ribozyme concentrations in the presence of 20 mM $MgCl_2$ for 1 h at 30 °C. The control lanes **a** and **b** show IL-6 mRNA (**a**) as a freshly prepared solution or (**b**) after 1 h of incubation without ribozyme. The lengths of the substrate (nucleotides) and the products are indicated at both sides.

gave the most stable structure (eight base pairs with one bulge in every helix) but also without formation of helix II. The other two ribozymes preferentially folded helix II together with a second duplex consisting of four base pairs. For the short substrates the same difference could be observed: Sub 674 formed five base pairs and therefore the most stable secondary structure among the substrates. In the other substrates hybridization of only two or three base pairs is observed. The improper folding of Rib 674 and its short substrate might partly explain its lower activity than the other complexes.

The long substrate, IL-6 mRNA, was obtained by run-off transcription of the pT7.7/IL-6 plasmid, containing the coding region of mature hIL-6 plus 445 bp of the 3′ untranslated sequence [12]. The ribozyme-mediated cleavage of the IL-6 mRNA only proceeded for Rib 418 and Rib 510 (Table 1; Figure 5). Rib 418 showed a decrease in catalytic efficiency to 1/300 of the activity on the short substrate, whereas for Rib 510 a decrease to only 1/30 was observed. Rib 674 did not show any cleavage activity at all, not even after preheating the ribozyme together with the IL-6 mRNA at 75 °C for 3 min followed by incubation for 1 h at 50 °C (results not shown). Rib 492 did not cleave owing to the presence of the uncleavable GUG triplet at the target site; it was therefore used as a control ribozyme (only antisense activity).

The most probable secondary structure of the IL-6 mRNA was determined by the method of Zuker [17] by using the FOLDRNA and SQUIGGLES software. Figure 6 shows that all amenable cleavage sites are located within comparable double-stranded regions. This calculated secondary structure therefore could not immediately reveal the reason for the remarkable differences in catalytic activity for the ribozymes.

DISCUSSION

IL-6 is a multifunctional cytokine involved mainly in the regulation of inflammatory and immunological processes [1]. Furthermore it seems to be important in the pathogenesis of several cancers and other diseases [2]. Inhibition or at least down-regulation of the IL-6 production might therefore be beneficial in the treatment of these often deadly diseases. Hammerhead

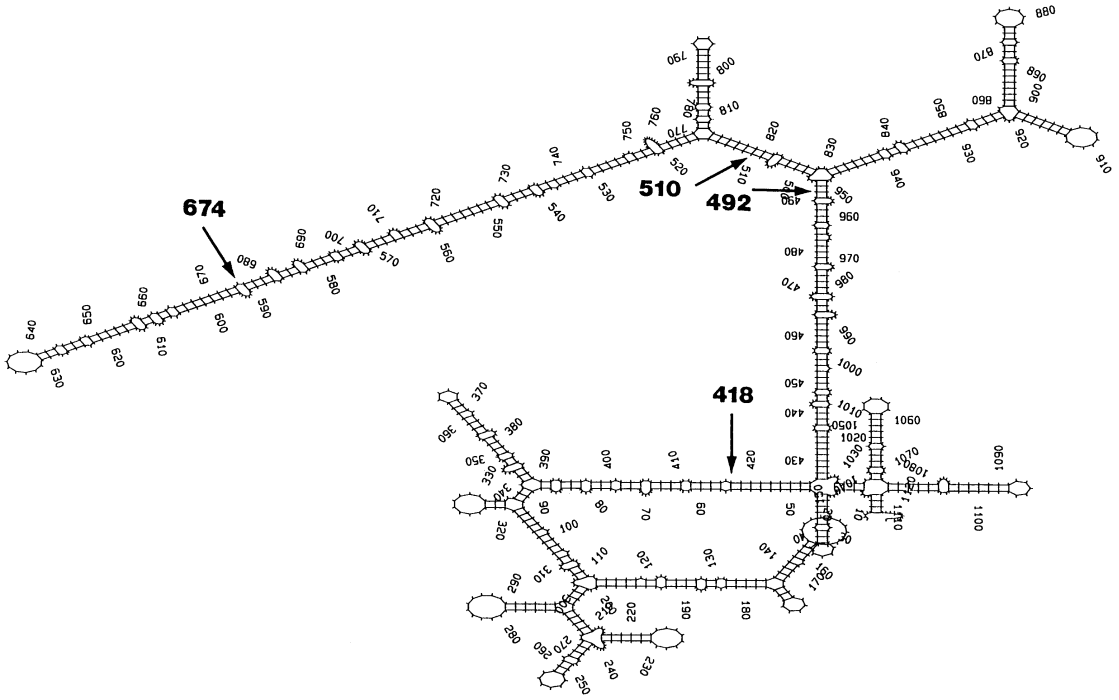

Figure 6 Secondary structure of the IL-6 mRNA as calculated by the FOLDRNA and SQUIGGLES software

Origin of the sequence: HSIFNβ2, M14584, SWISS-PROT Data Bank [9]. The cleavage sites at nucleotides 418, 492, 510 and 674 are indicated with arrows.

ribozymes, which can act as biological catalysts in cleaving a RNA substrate, could provide a more powerful alternative to antisense oligonucleotides. One of the problems associated with the use of ribozymes is the choice of the most suitable target site. It is quite comprehensible that not all potential target sites are equally accessible for ribozyme-mediated cleavage, because RNA conformations are stabilized by double-helical regions [28] and by other tertiary structures.

Cleavage by hammerhead ribozymes occurs preferentially after GUC sequences [6,7]. An important factor that determines the cleavage site is the south conformational preference of the carbohydrate moiety of the nucleotide [29]. Of all the 3′-ethylphosphate derivatives of the nucleotides, cytidine 3′-ethylphosphate demonstrates the highest preference for the south conformation. This preference indicates that cytidine, at the cleavage site of a hammerhead ribozyme, is more nearly at a transition state for the in-line attack at phosphorus than the other nucleotides [29]. The GUC sequence coding for residue 121 (Val) of the mature IL-6 protein sequence [18] has recently been used succesfully as a target for a hammerhead ribozyme [8]. However, according to the sequence provided by the SWISS-PROT Data Bank [9], human IL-6 mRNA contains four GUC sequences in the coding region (position of C at nucleotide 418, 492, 510 and 674) that are potentially amenable for hammerhead ribozyme-mediated cleavage [6,7]. The GUC triplet located at nucleotide 492 seems to be subject to polymorphism and appears as a GUC in IFNβ-2 mRNA, whereas in the sequences of hybridoma growth factor, 26,000 protein and B-cell stimulatory factor 2 it is replaced by a GUG [19], which is not a target for hammerhead ribozymes [6,7]. Our IL-6 mRNA transcript, obtained from the pT7.7/IL-6 plasmid [12], also has a GUG triplet in that position. Therefore the ribozyme designed to cleave this place was used as control in the cleavage experiments with the long mRNA substrate.

Targeting these four GUC triplets, hammerhead ribozymes and their respective short synthetic substrates (Figure 1) were synthesized. Preliminary comparative cleavage reactions (Figure 2) revealed that two of these ribozymes (Rib 492 and Rib 418) were distinctively more active than the other two (Rib 510 and Rib 674). Analysis of the initial velocities under multiple turnover conditions (Table 1) supported these results, which once more demonstrated the effect of substrate sequence [30] because these hammerheads contained identical catalytic core sequences but differed only in the base composition of the helices involved in substrate binding. Their K_m values showed only minor differences, which can be explained by evaluating the melting temperatures of the ribozyme–substrate complexes (Table 2 and Figure 3), because K_m is inversely related to the stability of the ribozyme–substrate hybrid. Indeed, Rib 674, which exhibits the lowest K_m value, has the highest melting temperature; the opposite can be observed for Rib 510. The variation in catalytic efficiency was mainly due to large differences in the $k_{cat.}$ values. The low activity of Rib 674 might be caused partly by its stable helices I and III, which limit the rate of product dissociation.

The secondary structure of the ribozymes and their short substrates was predicted by using the PC/Gene software (Figure 4; Table 2). All RNA strands adopt conformations that need to be disrupted to assemble ribozyme and short substrate into the proper hammerhead structure. Except for Rib 674 the stability of the ribozymes is achieved by the formation of duplexes between three or four base pairs that can easily be disrupted. The secondary structures formed by Rib 674 and by its short substrate are more stable than those observed for the other ribozymes. It might also be that intramolecular interactions hamper association of Rib 674 with a new substrate once the first target has been cleaved. Its lower efficiency could therefore be partly due to lower association and dissociation kinetics. However, calculation of the secondary structure of the ribozyme–substrate complex by making an imaginary connection between the 5′ or 3′ end of the ribozyme via a UUUU loop to its corresponding short substrate predicted the expected hammerhead structure for all the complexes, when using the free-energy values of Cech et al. [26]. With Freier's values [27], only the ribozyme–substrate complex 418 was predicted as a correct structure. All the other complexes folded improperly, lacking loop and helix II. Therefore, in our opinion, the free-energy values published by Cech et al. [26] seem to be more suitable for prediction of the secondary structure of these small RNA sequences because our experimental results can be partly explained by the data obtained by Cech's method.

The cleavage reactions on IL-6 mRNA revealed that only two ribozymes, Rib 418 and Rib 510, were able to cleave the 1035 nucleotides long substrate (Table 1; Figure 5). Compared with their activity on the short synthetic substrate, the catalytic efficiency of Rib 418 decreased to 1/300, for Rib 510, however, only a decrease to 1/30 was observed. These results show less dramatic difference between activity on short compared with long substrates than previously reported for the cleavage of a long substrate of similar length, where the cleavage of the HIV-1 LTR RNA transcript of 985 nucleotides was generally more than three orders of magnitude less efficient than corresponding short synthetic substrates [14]. As expected, the control ribozyme, Rib 492, did not cleave the long mRNA substrate. In contrast, the total lack of activity of Rib 674 on the long substrate was surprising. According to the most probable secondary structure of the IL-6 mRNA (Figure 6), the target sites are all located in double-stranded regions, which seem very much alike. Closer examination of the base composition of these regions, however, indicates that from these sites, the sequence targeted by Rib 674 contains the highest number of GC base pairs. This target site may therefore be so stable that it fails to exchange into a cleavable substrate on the time scale of the reaction, and seems to be inert to the ribozyme attack. This, together with the above-mentioned higher stability of Rib 674 owing to intramolecular interactions, may explain the inactivity of Rib 674.

In summary, this study confirms that an examination of the duplex stability between ribozyme and substrate together with an analysis of possible intramolecular association might be useful during the selection procedure of an active ribozyme. The study also indicates that the GUC triplet located at nucleotide 510 on the mRNA of IL-6 is probably the best site for hammerhead ribozyme-mediated cleavage. Because it has earlier been demonstrated that this site can also be successfully targeted in cellular systems [8], we shall in future use this location as an amenable target for cleavage by chemically modified hammerhead ribozymes.

We thank Dr. J. Content and M. Mahieu for the gift of the pT7.7/IL-6 expression plasmid; G. Schepers for synthesis of the oligonucleotides; Dr. L. Van Mellaert for her kind explanations; Dr. G. Opdenakker for the use of the scanning laser densitometer and for helpful discussions; and P. Fiten and Dr. J. Rozenski for their indispensable help in computer manipulations. A.V.A. and B.J. are research associates of the Belgian National Fund of Scientific Research.

REFERENCES

1 Van Snick, J. (1990) Annu. Rev. Immunol. **8**, 253–278
2 Hirano, T., Akira, S., Taga, T. and Kishimoto, T. (1990) Immunol. Today **11**, 443–449
3 Wolvekamp, M. C. J. and Marquet, R. L. (1990) Immunol. Lett. **24**, 1–10
4 Bauer, J. and Herrmann, F. (1991) Ann. Hematol. **62**, 203–210

5 Uhlenbeck, O. C. (1987) Nature (London) **328**, 596–600
6 Haseloff, J. and Gerlach, W. L. (1988) Nature (London) **334**, 585–591
7 Ruffner, D. E., Stormo, G. D. and Uhlenbeck, O. C. (1990) Biochemistry **29**, 10695–10702
8 Mahieu, M., Deschuyteneer, R., Forget, D., Vandenbussche, P. and Content, J. (1994) Blood **84**, 3758–3765
9 May, L. T., Helfgott, D. C. and Sehgal, P. B. (1986) Proc. Natl. Acad. Sci. U.S.A. **83**, 8957–8961
10 Tang, J. Y., Guo, Q., Roskey, A. and Agrawal, S. (1993) J. Cell. Biochem. **17**, 214 (S417)
11 Hendrix, C., Devreese, B., Rozenski, J., Van Aerschot, A., De Bruyn, A., Van Beeumen, J. and Herdewijn, P. (1995) Nucl. Acids Res. **23**, 51–57
12 Arcone, R., Pucci, P., Zappacosta, F., Fontaine, V., Malorni, A., Marino, G. and Ciliberto, G. (1991) Eur. J. Biochem. **198**, 541-547
13 Fersht, A. (1985) Enzyme structure and mechanism, W. H. Freeman and Co., New York
14 Heidenreich, O. and Eckstein, F. (1992) J. Biol. Chem. **267**, 1904–1909
15 Heidenreich, O., Benseler, F., Fahrenholz, A. and Eckstein, F. (1994) J. Biol. Chem. **269**, 2131–2138
16 Augustyns, K., Godard, G., Hendrix, C., Van Aerschot, A., Rozenski, J., Saison-Behmoaras, T. and Herdewijn, P. (1993) Nucleic Acids Res. **21**, 4670–4676
17 Zuker, M. (1989) Methods Enzymol. **180**, 262–288
18 Hirano, T., Yasukawa, K., Harada, H., Taga, T., Watanabe, Y., Matsuda, T., Kashiwamura, S., Nakajima, K., Koyama, K., Iwamatsu, A., Tsunasawa, S., Sakiyama, F., Matsui, H., Takahara, Y., Taniguchi, T. and Kishimoto, T. (1986) Nature (London) **324**, 73–76
19 Brakenhoff, J. P. J., de Groot E. R., Evers, R. F., Pannekoek, H. and Aarden, L. A. (1987) J. Immunol. **139**, 4116–4121
20 Heus, H. A. and Pardi, A. (1991) Science **253**, 191–194
21 SantaLucia, J., Jr., Kierzek, R. and Turner, D. H. (1992) Science **256**, 217–219
22 Seela, F. and Kaiser, K. (1987) Nucleic Acids Res. **15**, 3113–3129
23 Temsamani, J., Tang, J.-Y., Padmapriya, A., Kubert, M. and Agrawal, S. (1993) Antisense Res. Dev. **3**, 277–284
24 Hendrix, C., Mahieu, M., Anné, J., Van Calenbergh, S., Van Aerschot, A., Content, J. and Herdewijn, P. (1995) Biochem. Biophys. Res. Commun. **210**, 67–73
25 Zuker, M. and Stiegler, P. (1981) Nucleic Acids Res. **9**, 133–148
26 Cech, T. R., Tanner, N. K., Tinoco, I. Jr., Weir, B. R., Zuker, M. and Perlman, P. S. (1983) Proc. Natl. Acad. Sci. **80**, 3903-3907
27 Freier, S. M., Kierzek, R., Jaeger, J. A., Sugimoto, N., Caruthers, M. H., Neilson, T. and Turner, D. H. (1986) Proc. Natl. Acad. Sci. U.S.A. **83**, 9373–9377
28 Saenger, W. (1984) Principles of Nucleic Acid Structure, Springer-Verlag, New York
29 Plavec, J., Thibaudeau, C. and Chattopadhyaya, J. (1994) J. Am. Chem. Soc. **116**, 6558–6560
30 Fedor, M. J. and Uhlenbeck, O. C. (1990) Proc. Natl. Acad. Sci. U.S.A. **87**, 1668–1672
31 Hertel, K. J., Pardi, A., Uhlenbeck, O. C., Koizumi, M., Ohtsuka, E., Uesugi, S., Cedergren, R., Eckstein, F., Gerlach, W. L., Hodgson, R. and Symons, R. H. (1992) Nucleic Acids Res. **20**, 3252

Received 15 September 1995/25 October 1995; accepted 2 November 1995